Table 3.1.1
Aberrations comprising the geometric component of the IPF

Aberration	Controlling parameters	Impact
X-ray source width (w_x)	Angle subtended by source: w_x/R	Symmetric broadening
Receiving-slit width or PSD strip width (w_r)	Angle subtended by slit/strip: w_r/R	Symmetric broadening
Flat specimen error/equatorial divergence	Angle of divergence slit: α	Asymmetric broadening to low 2θ, with decreasing 2θ
PSD defocusing	PSD window width, angle of divergence slit: α	Symmetric broadening with $1/(\tan\theta)$
Axial divergence Case 1: no Soller slits Case 2: Soller slits define divergence angle	 Axial lengths of the X-ray source (L_x), sample (L_s) and receiving slit (L_r) relative to goniometer radius (R) Acceptance angles Δ_I and Δ_D of the incident- and diffracted-beam Soller slits	Below $\sim 100°$: asymmetric broadening to low 2θ, with decreasing 2θ else to high 2θ, with increasing 2θ
Specimen transparency	Penetration factor relative to diffractometer radius $1/\mu R$	Asymmetric broadening to low 2θ, with $\sin(2\theta)$
Specimen displacement z height	Displacement of specimen surface from goniometer rotation axes	Displacement of profiles with $\cos\theta$

side of Fig. 3.1.3. In this way, a Johansson optic provides a monochromatic X-ray source, passing some portion of the $K\alpha_1$ emission spectrum, while preserving the divergent-beam Bragg–Brentano geometry as shown in Figs. 3.1.1 and 3.1.2. The use of an IBM reduces the number of spectral contributions to the observed line shape and results in an IPF that is more readily modelled with conventional profile fitting. Furthermore, equipping such a machine with a PSD affords all of its advantages, while the elimination of the *Bremsstrahlung* by the IBM reduces the impact of fluorescence that can otherwise be problematic with a PSD.

Throughout this manuscript we use the terms 'width' and 'length' when referring to the optics. Width expresses extent in the equatorial plane. Length is used to denote a physical dimension parallel to the rotation axes of the goniometer as defined in Fig. 3.1.1. The designation of the axial divergence angle, as well as the specifications concerning Soller slits, will be considered in terms of the double angle, both for incoming and outgoing X-rays. This is in contrast to the generally accepted single-angle definition shown in Klug & Alexander (1974); hence the axial-divergence angles reported throughout this chapter are twice those that are often encountered elsewhere.

The observed line shape in powder diffraction consists of a convolution of contributions from the instrument optics (referred to as the geometric profile), the emission spectrum and the specimen, as shown diagrammatically for divergent-beam XRPD in Fig. 3.1.4. The specimen contribution is often the dominant one in a given experiment; however, we do not consider it to any great extent in this discussion. The factors comprising the geometric profile are listed in Table 3.1.1. Technically, neither of the last two items (specimen transparency and displacement) are components of the geometric profile of the instrument. They are functions of the specimen and the manner in which it was mounted. However, it is not possible to use a whole-pattern data-analysis method without considering these two factors; as they play a critical role in the modelling of the observed profile positions and shapes they are included in this discussion. The convolution of the components of the geometric profile and emission spectrum forms the IPF. As will be discussed, both of these contributions are complex in nature, leading to the well known difficulty in modelling the IPF from Bragg–Brentano equipment. This complexity, and the relatively limited q-space (momentum space) range accessible with laboratory equipment, tends to drive the structure solution and refinement community, with their expertise in the development of data-analysis procedures, towards the use of synchrotron and neutron sources. A significant number of the models and analytical functions discussed here were developed for, and are better suited to, powder-diffraction equipment using such nonconventional sources.

We now consider the geometric profile with an examination of the aberrations listed in Table 3.1.1. Figs. 3.1.5–3.1.10 illustrate simulations of the aberration function associated with the factors listed in Table 3.1.1. The first two of these, the source and receiving-slit width or silicon strip width with a PSD, simply cause symmetric broadening, constant with 2θ angle, and are typically described with 'impulse' or 'top-hat' functions. The flat specimen error is due to defocusing in the equatorial plane. One can see from Fig. 3.1.1 that for any beam that is not on the centre line of the goniometer, R_1 is not equal to R_2. The magnitude of the effect is directly

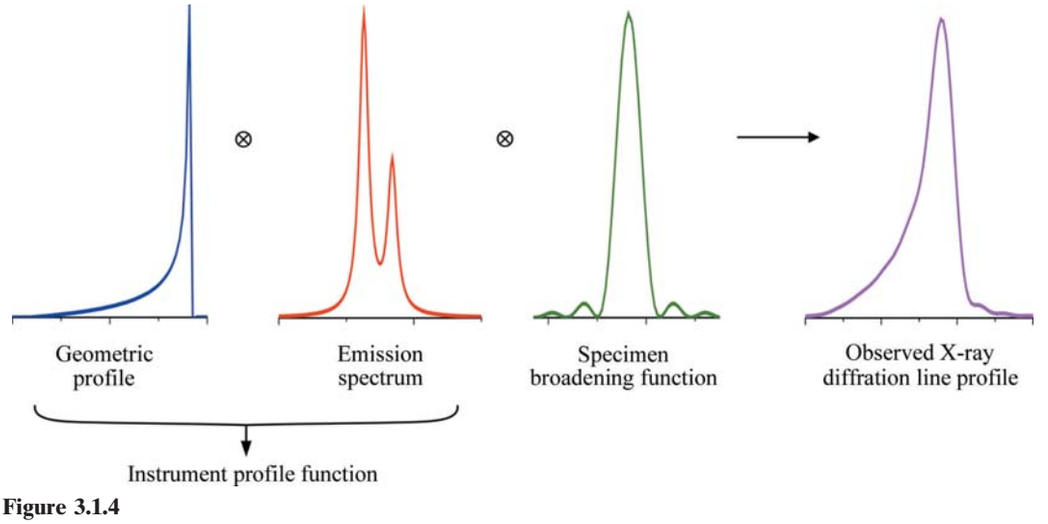

Figure 3.1.4
Diagrammatic representations of convolutions leading to the observed XRPD profile.